

Load Balancing for Massively Parallel Transport Sweeps on Unstructured Meshes

Tarek H. Ghaddar,* Jean C. Ragusa*

**Dept. of Nuclear Engineering, Texas A&M University, College Station, TX, 77843-3133
tghaddar@tamu.edu, jean.ragusa@tamu.edu*

INTRODUCTION

When running any massively parallel code, load balancing is a priority in order to achieve the best possible parallel efficiency. A load balanced problem has an equal number of degrees of freedom per processor. Load balancing is important in order to minimize idle time for all processors by equally distributing (as much as possible) the work load for each processor. **add a notation about communications too**

directly hit with transport sweeps but with logically Cartesian grids The concepts and results presented in this paper are used by PDT, Texas A&M University's massively parallel deterministic transport code. It is capable of multi-group simulations and employs discrete ordinates for angular discretization, and utilizes transport sweeps to solve the transport equation for neutron, thermal, gamma, coupled neutron-gamma, electron, and coupled electron-photon radiation. To the best of our knowledge, transport sweeps are the only stuff to scale on current and next generation machines. PDT has been shown to scale on logically Cartesian grids out to 750,000 cores[1]. Logically Cartesian grids contain regular convex grid units that allow for vertex motion inside them in order to conform to curved shapes. **then PDT**

A new unstructured meshing capability was implemented in PDT in order to realistically represent certain geometries. Cut lines (planes for 3D cases) are used to partition the geometry into **logically-Cartesian** subdomains, which are then individually meshed in parallel using the Triangle Mesh Generator[2]. These subdomains are then "stitched" together in order to create a continuous geometry. 2D meshes can be extruded in the z dimension for 3D problems.

Unstructured meshes create unbalanced problems due to the way localized features can be meshed, so a load balancing algorithm was added into PDT. A load balanced problem is determined by the value of f , where f is the subset with the maximum number of cells, divided by the average number of cells per subset. A perfectly balanced problem has $f = 1$.

APPLICATION OF 2D AND 3D UNSTRUCTURED MESHES

The capability for PDT to generate and run on an unstructured mesh is important because it allows us to run problems without having to conform our mesh to the problem as much. The idea is to have a logically Cartesian grid (creating orthogonal "subsets") with an unstructured mesh inside each subset. These logically Cartesian subdomains are obtained using cut planes in 3D and cut lines in 2D. Figure 1 demonstrates this functionality. It is decomposed into 3 subsets in x and 3 in y, with the first two subsets meshed using the Triangle Mesh Generator[2], a 2D mesh generator.

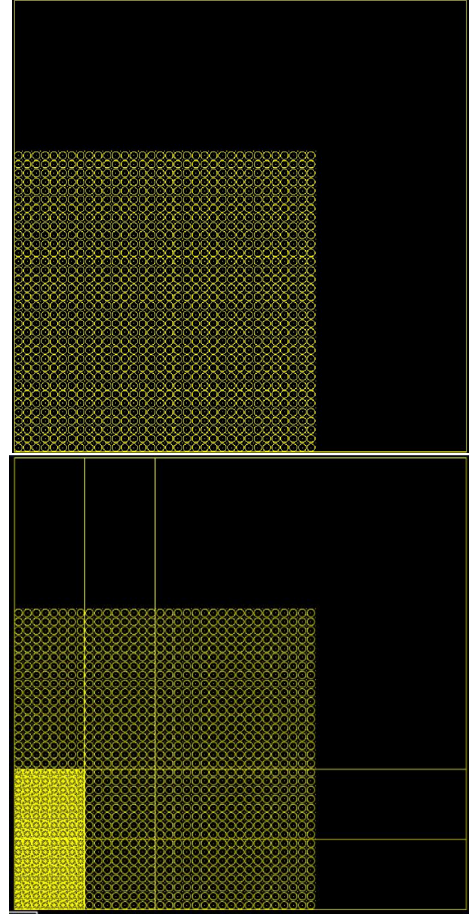


Fig. 1. A PSLG describing a fuel lattice, and with an orthogonal "subset" grid imposed on the PSLG.

This orthogonal grid is superimposed and each subset is meshed in parallel. Subsets are now the base structured unit when calculating our parallel efficiency. Discontinuities along the boundary are fixed by "stitching" hanging nodes, creating degenerate polygons along subset boundaries. Because PDT's spatial discretization employs Piece-Wise Linear Discontinuous (PWLD) finite element basis functions, there is no problem solving on degenerate polygons.

When using the unstructured meshing capability in PDT, the input geometry is described by a Planar Straight Line Graph (PSLG). After superimposing the orthogonal grid, a PSLG is created for each subset, and meshed. Because the input's and each subset's PSLG must be described and meshed in 2D, the mesh can be extruded in the z dimension in order to give us the capability to run on 3D problems. Obviously, this is not as good as an unstructured tetrahedral mesh, but for many problems, it is a great capability to have.

To showcase, the newly implemented unstructured meshing capability in PDT, Texas A&M Nuclear Engineering's Impurity Model 1 (IM1) problem is used. Figure 2 showcases the 2D mesh of the IM1 problem,

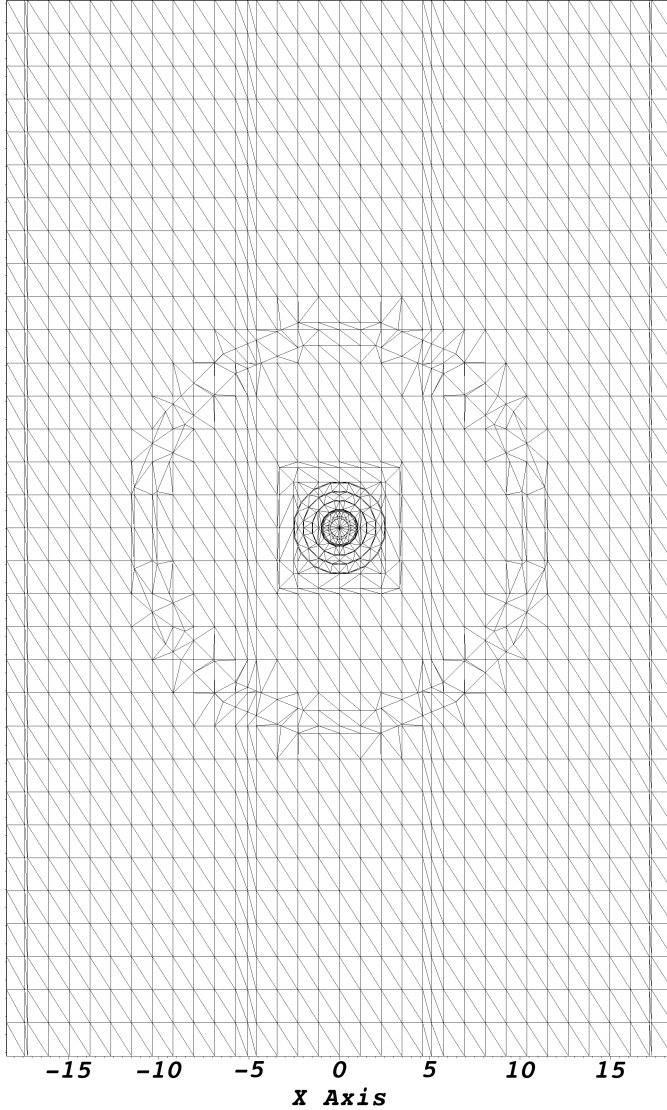


Fig. 2. The 2D mesh of the IM1 problem.

In order to get from the 2D mesh to the 2D extruded mesh, an extrusion file is supplied to PDT. This extrusion file supplies two critical pieces of information: the number of z layers and their locations, and how each region of the 2D mesh is mapped to these z layers. The combination of the 2D mesh and the extrusion file yield the full 3D problem, shown in Fig. 3.

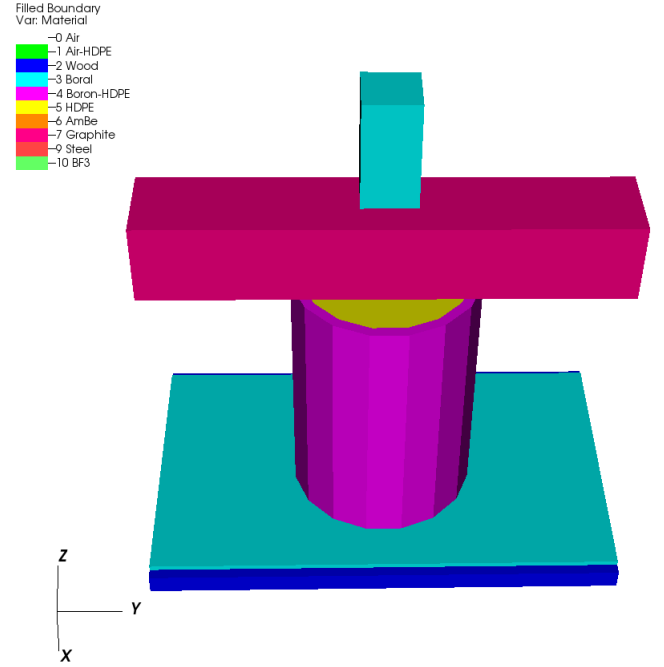


Fig. 3. The 2D extruded view of the IM1 problem.

THE LOAD BALANCING ALGORITHM

not sure we this this paragraph When discussing the parallel scaling of transport sweeps, a load balanced problem is of great importance. A load balanced problem has an equal number of degrees of freedom per processor. Load balancing is important in order to minimize idle time for all processors by equally distributing (as much as possible) the work each processor has to do. For the purposes of unstructured meshes in PDT, we are looking to “balance” the number of cells. Ideally, each processor will be responsible for an equal number of cells.

re-emphasize that this is done in the context of the provably-optimal transport sweep on logically Cartesian grids, hence your desire to equally spread the DoFs in the subsets If the number of cells in each subset can be reasonably balanced, then the problem is effectively load balanced. The Load Balance algorithm described below details how the subsets will be load balanced. In summary, the procedure of the algorithm involves moving the initially user specified x and y cut planes, re-meshing, and iterating until a reasonably load balanced problem is obtained. Equation 1 shows the equation for calculating the load balancing metric, which dictates how balanced or unbalanced the problem is.

$$f = \frac{\max_{ij}(N_{ij})}{\frac{N_{tot}}{I \cdot J}}, \quad (1)$$

where f is the load balance metric, N_{ij} is the number of cells in subset i, j , N_{tot} is the global number of cells in the problem,

and I and J are the total number of in the x and y direction, respectively. The metric is a measure of the maximum number of cells per subset divided by the average number of cells per subset.

The load balancing algorithm moves cut planes based on two sub-metrics, f_I and f_J . Equation (2) defines these two parameters:

$$f_I = \frac{\max_i [\sum_j N_{ij}]}{\frac{N_{tot}}{I}} \quad (2a)$$

$$f_J = \frac{\max_j [\sum_i N_{ij}]}{\frac{N_{tot}}{J}}. \quad (2b)$$

f_I is calculated by taking the maximum number of cells per column and dividing it by the average number of cells per column. f_J is calculated by taking the maximum number of cells per row and dividing it by the average number of cells per row. If these two numbers are greater than predefined tolerances, the cut lines in the respective directions are redistributed. Once redistribution and remeshing occur, a new metric is calculated. This iterative process occurs until a maximum number of iterations is reached, or until f converges within the user defined tolerance. The Load Balance algorithm behaves as follows:

```
//I, J subsets specified by user
//Check if all subsets meet the tolerance
while (f > tol_subset)
{
    //Mesh all subsets
    if (f_I > tol_column)
    {
        Redistribute(X);
    }
    if (f_J > tol_row)
    {
        Redistribute(Y);
    }
}
```

RESULTS

The following sections will showcase the metric behavior and convergence for three test cases and the new unstructured meshing capability both in 2D and 3D.

Test Cases for Metric Behavior and Convergence

In order to showcase the behavior of the load balancing metric, calculated by Eq. 1 three test cases are presented. Figure 4 shows the first test case, a 20 cm by 20 cm domain with two pins in opposite corners of the domain. Figure 5 shows the same size domain but with the pins on the same side. These are two theoretically very unbalanced cases, as geometrically there are two features located distantly from each other with an empty geometry throughout the rest of the domain. Figure 6 shows a lattice and reflector, which due to its denser and repeated geometry, theoretically is a more balanced problem.

A series of 162 inputs was constructed for each case. These inputs are constructed by varying the maximum triangle

Redistribute: A function that moves cut lines in either X or Y.

Input: CutLines (X or Y vector that stores cut lines).

Input: num_tri_row or num_tri_col, a pArray containing number of triangles in each row or column

Input: The total number of triangles in the domain, N_{tot}
 stapl::array_view num_tri_view, over num_tri_row/column
 stapl::array_view offset_view
 stapl::partial_sum(num_tri_view) {Perform prefix sum}
 {We now have a cumulative distribution stored in offset_view}

for $i = 1 : \text{CutLines.size}() - 1$ **do**

vector <double> pt1 = [CutLines(i-1), offset_view(i-1)]

vector <double> pt2 = [CutLines(i), offset_view(i)]

ideal_value = $i \cdot \frac{N_{tot}}{\text{CutLines.size}() - 1}$

X-intersect(pt1, pt2, ideal_value) {Calculates the X-intersect of the line formed by pt1 and pt2 and the line $y = \text{ideal_value}$.}

CutLines(i) = X-intersect

end for

area from the coarsest possible to 0.01 cm² and the number of subsets, N from 2×2 to 10×10.

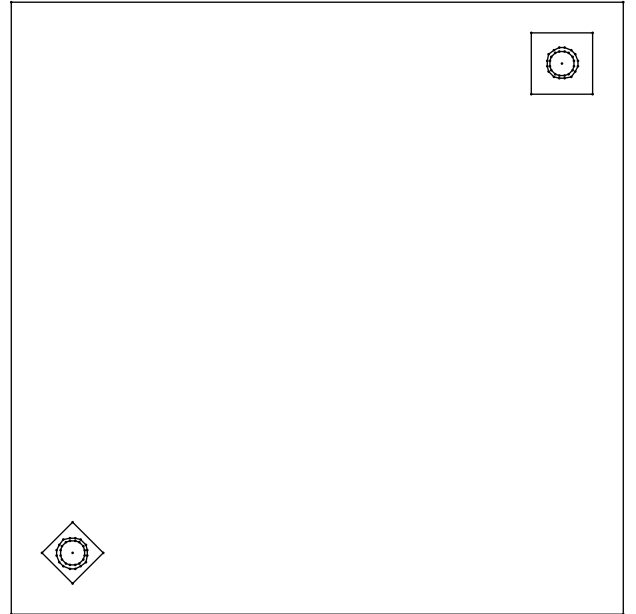


Fig. 4. The first test case used in order to test effectiveness and convergence of the load balancing metric.

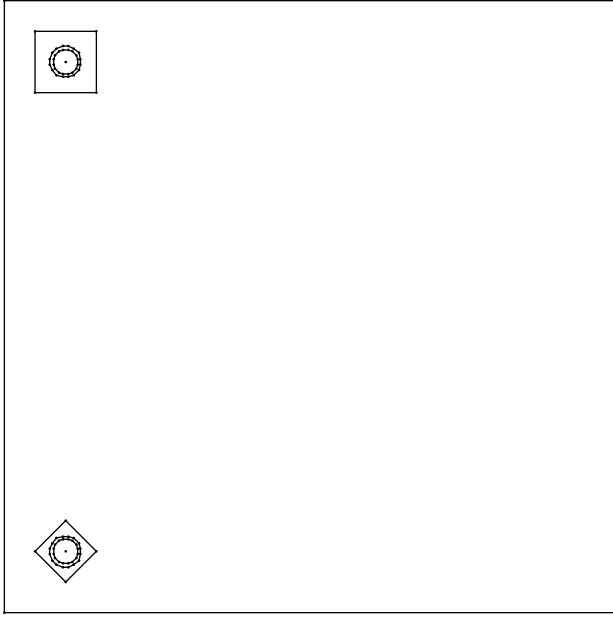


Fig. 5. The second test case used in order to test effectiveness and convergence of the load balancing metric.

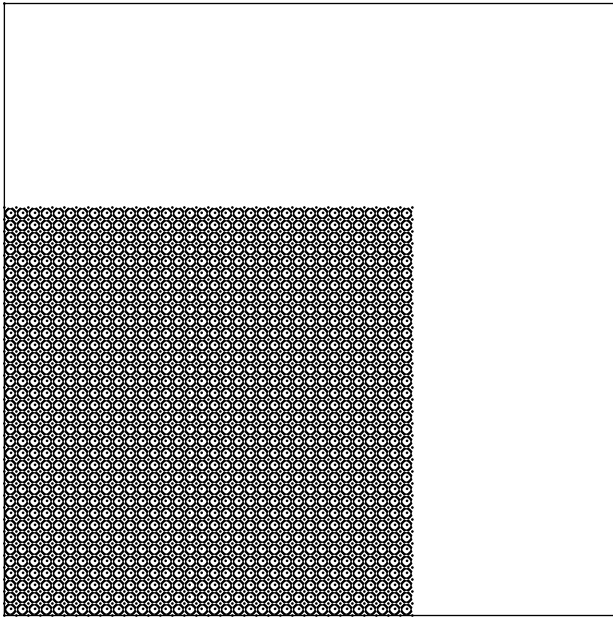


Fig. 6. The third test case used in order to test effectiveness and convergence of the load balancing metric.

Metric Behavior and Convergence

For each test case, the 162 input inputs are run twice, once with no load balancing iterations, and once with ten load balancing iterations. The best metric is reported and recorded. Three figures for each test cases are presented below: the first figure will show the metric behavior for no iterations, the second figure will show the metric behavior for each input

run with ten load balancing iterations, and the third figure will show a ratio of the ten iteration runs over the no iteration runs.

Figure 7 shows the metric behavior for Fig. 4. The maximum metric value is 24.7650, and occurs when Fig. 4 is run with 8x8 subsets and a maximum triangle area of 1.6 cm². The minimum metric value is 1.0016 and occurs when Fig. 4 is run with 4x4 subsets and a maximum triangle area of 0.04 cm².

Metric Behavior with no Load Balancing Iterations

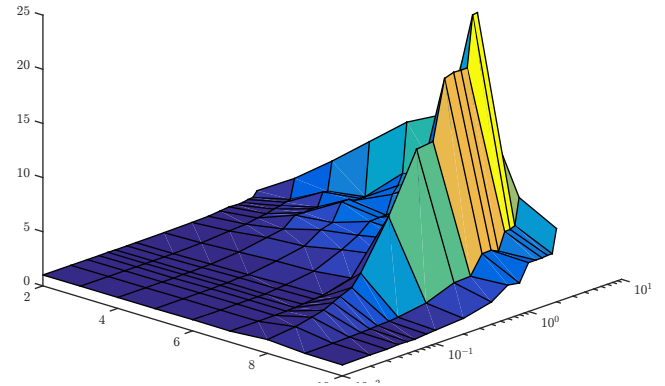


Fig. 7. The metric behavior of the first test case run with no load balancing iterations.

Figure 8 shows the metric behavior for Fig. 4 after 10 load balancing iterations. The maximum metric value is 5.0538 and occurs when Fig. 4 is run with 10x10 subsets and a maximum triangle area of 1.2 cm². The minimum metric value is 1.0017 and occurs when Fig. 4 is run with 4x4 subsets and a maximum triangle area of 0.04 cm².

Metric Behavior with 10 Load Balancing Iterations

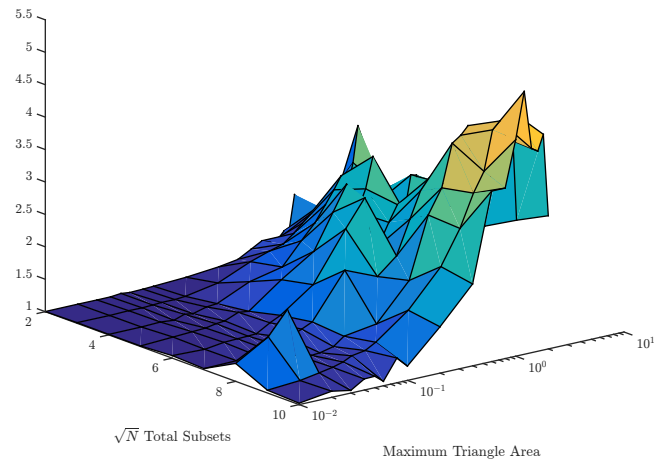


Fig. 8. The metric behavior of the first test case run with 10 load balancing iterations.

Figure 9 shows the metric behavior for Fig. 5. The maximum metric is 22.6654 and occurs when Fig. 5 is run with

8x8 subsets with a maximum triangle area of 1.8 cm^2 . The minimum metric is 1.0024 and occurs when Fig. 5 is run with 2x2 subsets with a maximum triangle area of 0.01 cm^2 .

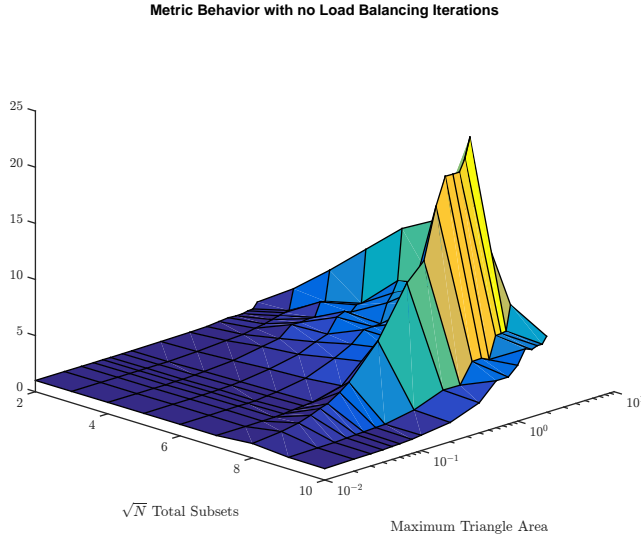


Fig. 9. The metric behavior of the second test case run with no load balancing iterations.

Figure 10 shows the metric behavior for Fig. 5 after ten load balancing iterations. The maximum metric is 3.9929 and occurs when Fig. 5 is run with 10x10 subsets with a maximum triangle area of 1.8 cm^2 . The minimum metric is 1.0024 and occurs when Fig. 5 is run with 2x2 subsets with a maximum triangle area of 0.01 cm^2 .

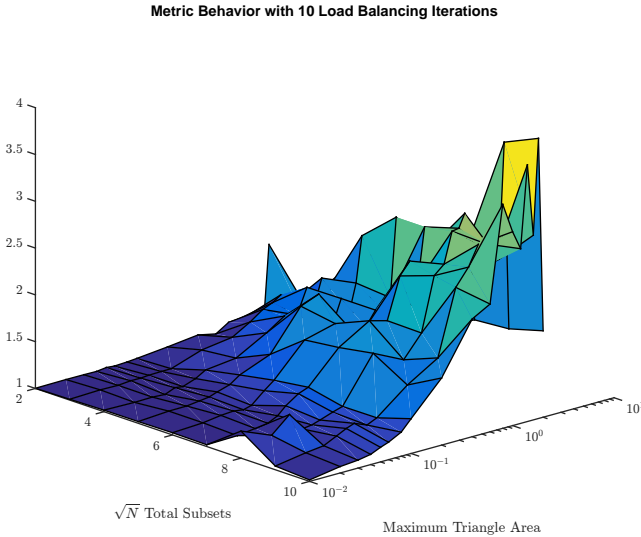


Fig. 10. The metric behavior of the second test case run with 10 load balancing iterations.

Figure 11 shows the metric behavior for Fig. 6. The maximum metric is 2.6489 and occurs when Fig. 6 is run with 10x10 subsets with a maximum triangle area of 1.8 cm^2 . The

minimum metric is 1.0179 and occurs when Fig. 6 is run with 2x2 subsets with a maximum triangle area of 0.08 cm^2 .

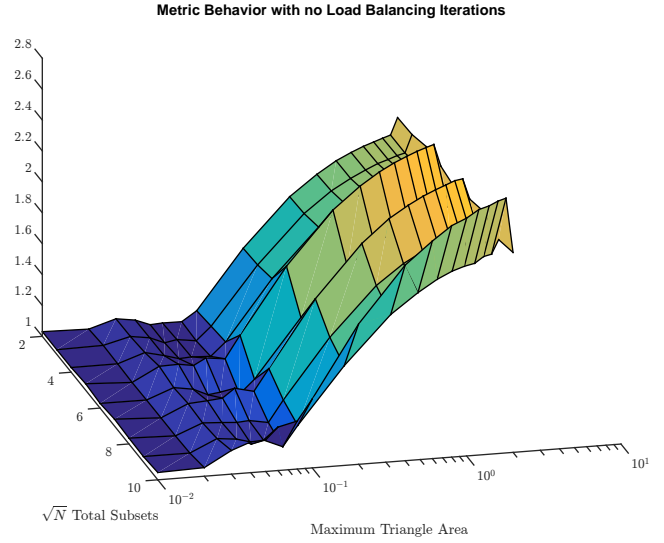


Fig. 11. The difference in metric behavior of the third test case with no load balancing iterations.

Figure 12 shows the metric behavior for Fig. 6 after ten load balancing iterations. The maximum metric is 2.2660 and occurs when Fig. 6 is run with 10x10 subsets with a maximum triangle area of 0.4 cm^2 . The minimum metric is 1.0021 and occurs when Fig. 6 is run with 2x2 subsets with the Triangle's coarsest possible mesh.

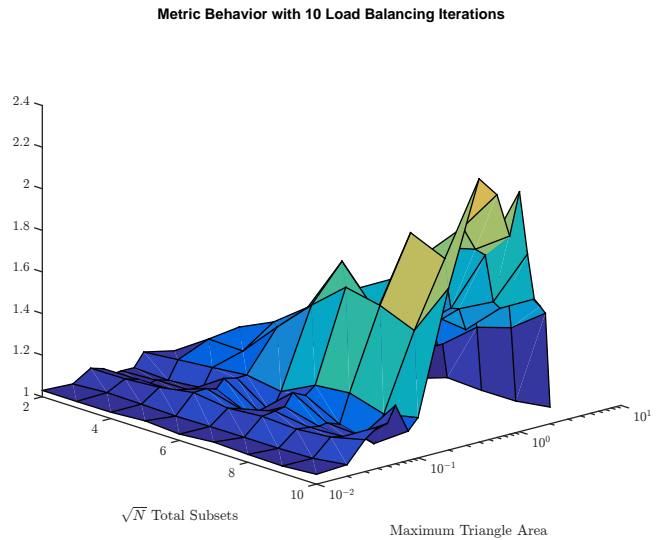


Fig. 12. The difference in metric behavior of the third test case after ten load balancing iterations.

Because Fig. 6 has more features and is more symmetric of a problem, the initial load balancing metric will not be as large as the load balancing metric of Figs. 5 and 4. As a result, the improvement in the load balancing metric after 10

iterations will not be as great in problems similar to Fig. 6.

Good improvement is seen throughout all three test cases for all three inputs, particularly the first two test cases, which were initially very unbalanced. However, there were many inputs run that had problems with $f > 1.1$, which means many problems were unbalanced by more than 10%. The user will not always have the luxury of choosing the number of subsets they want the problem run with, as this directly affects the number of processors the problem will be run with. Certain problems will require more processors and will require minimizing the total number of cells in the domain for the problem to complete running in a reasonable amount of time. As a result, improvements to the algorithm must be made.

This can be done by changing how the cut lines are redistributed. Instead of changing entire row and column widths, the cut lines can be moved on the subset level. However, this can sacrifice the strict orthogonality that PDT currently utilizes to scale so well on a massively parallel scale. Changes to the performance model and the scheduler would have to be made.

Another option is to implement domain overloading, which is the logical extension of the work presented in this paper. This would involve processors owning different numbers of subsets, with no restriction on these subsets being contiguous. This would be the most effective method at perfecting this algorithm, and would lead to less problems being unbalanced by more than 10%.

CONCLUSIONS

In conclusion, the load balancing algorithm outlined in this paper performs satisfactorily for more symmetric problems with a lot of geometrical features, and even for particularly unbalanced problems. As shown in [Chapter](#), its effectiveness depends on the maximum triangle area used and the number of subsets chosen to decompose the problem domain.

Load imbalance reduction is observed throughout all three test cases for all three inputs, particularly the first two test cases, which were initially very unbalanced. However, there were many inputs run that had problems with $f > 1.1$, which means many problems were unbalanced by more than 10%. It is not always to chosen the number of subsets as this directly affects the number of processors the problem will be run with. Certain problems will require more processors and will require minimizing the total number of cells in the domain for the problem to complete running in a reasonable amount of time. As a result, improvements to the algorithm must be made.

This can be done by changing how the cut lines are redistributed. Instead of changing entire row and column widths, the cut lines can be moved on the subset level. However, this can sacrifice the strict orthogonality that PDT currently utilizes to perform transport sweep on a massively parallel scale.

ACKNOWLEDGMENTS

REFERENCES

1. M. A. ET AL, "Provably Optimal Parallel Transport Sweeps with Non-Contiguous Partitions," in "ANS MC2015-Joint International Conference on Mathematics

and Computation (M&C), Supercomputing in Nuclear Applications (SNA) and the Monte Carlo (MC) Method," (2015).

2. J. SHEWCHUK, "Triangle: Engineering a 2D Quality Mesh Generator and Delaunay Triangulator," in M. C. LIN and D. MANOCHA, editors, "Applied Computational Geometry: Towards Geometric Engineering," Springer-Verlag, *Lecture Notes in Computer Science*, vol. 1148, pp. 203–222 (May 1996), from the First ACM Workshop on Applied Computational Geometry.